NANO LETTERS

2007
Vol. 7, No. 10
2960−2965

Gallium Phosphide Nanowires as a Substrate for Cultured Neurons

Waldemar Hällström,*,† Thomas Mårtensson,† Christelle Prinz,† Per Gustavsson,‡ Lars Montelius,† Lars Samuelson,† and Martin Kanje‡

Division of Solid State Physics & The Nanometer Structure Consortium, Lund University, P.O Box 118, 221 00 Lund, Sweden, Cell and Organism Biology, Lund University, Sweden

Received March 28, 2007; Revised Manuscript Received July 25, 2007

ABSTRACT

Dissociated sensory neurons were cultured on epitaxial gallium phosphide (GaP) nanowires grown vertically from a gallium phosphide surface. Substrates covered by 2.5 μm long, 50 nm wide nanowires supported cell adhesion and axonal outgrowth. Cell survival was better on nanowire substrates than on planar control substrates. The cells interacted closely with the nanostructures, and cells penetrated by hundreds of wires were observed as well as wire bending due to forces exerted by the cells.

One of the greatest possibilities of micro- and nanotechnology lies in cell research and life sciences at the cellular and subcellular level. This is natural because almost all activities of cells, which are around 10 μm in diameter, take place at the micrometer or submicrometer scale. Recent achievements in this field include the construction of structures for cell guidance and cell adhesion, registration of electrical activity in neurons, studies of the mechanical properties of cells, introducing macromolecules into the cell, or constraining cellular movement.[1−11] In particular, carbon nanotubes on surfaces have shown to promote neurons attachment and survival.[12,13] Functionalized carbon nanotube surfaces and carbon nanotube composites are permissive substrates for neurite outgrowth.[14,15]

Recent advances in nanotechnology have enabled well-controlled bottom-up fabrication of high-aspect-ratio nanostructures such as nanowires[16] as well as their controlled lateral assembly using prepatterning by electron beam lithography (EBL) and nanoimprint lithography (NIL).[17] The versatility of nanowires makes them very interesting building blocks in nanoscience: the semiconductor composition can be altered to create heterostructures, making it possible to tailor the band structure and electronic properties of the wire.[18] The nanowire surface can be functionalized, and with its high surface-to-volume ratio, they are ideal as highly sensitive chemical sensors.[19] Also, the morphology alone makes them interesting for probing applications because structures with such high aspect ratio are hard to produce using traditional top-down etching methods, especially if electronic function is to be retained. The present study addresses how cells and, in particular, sensory neurons interact with nanowires.

A commonly used nanowire growth method is the so-called vapor−liquid−solid (VLS) or, in other cases, the vapor−solid−solid (VSS) growth mode, where the nanowires grow with the aid of a catalytic gold particle.[20−22] Using metal−organic vapor-phase epitaxy (MOVPE) together with this catalytic growth mechanism, a number of III/V materials can be grown to form nanowires on various III/V substrates. III/V nanowires can also be grown on Si surfaces,[23] which increase the range of their applicability. With this method, the wires are monolithically integrated with the substrate, and their direction, diameter, and length can be carefully controlled.[24] Also, large-scale patterning with site control of individual nanowires can be achieved by EBL or NIL.[17]

Gallium phosphide (GaP) is a hard, semitransparent III/V semiconductor with well-characterized electrical and optical properties.[25] The properties in biochemical and biological environments are however much less known, as is the biocompatibility of the material. Nearly perfect GaP nanowires can be grown on a GaP substrate.[26] Therefore it is of interest to investigate whether GaP nanowires may be a suitable candidate for bioapplications. However, if nanodevices are to be used for cell probing, an important requirement is that they are biocompatible or, at least, not cytotoxic. In this study, we raised the question if neurons could attach, survive, and extend axons on planar GaP surfaces and on GaP surfaces endowed with nanowires. If so, how would the wire/cell interactions look like?

Substrates of planar GaP and substrates of GaP with nanowires were prepared and compared to untreated glass.

* Corresponding author. E-mail: waldemar.hallstrom@ftf.lth.se.
† Division of Solid State Physics & The Nanometer Structure Consortium.
‡ Cell and Organism Biology.

10.1021/nl070728e CCC: $37.00
Published on Web 09/19/2007

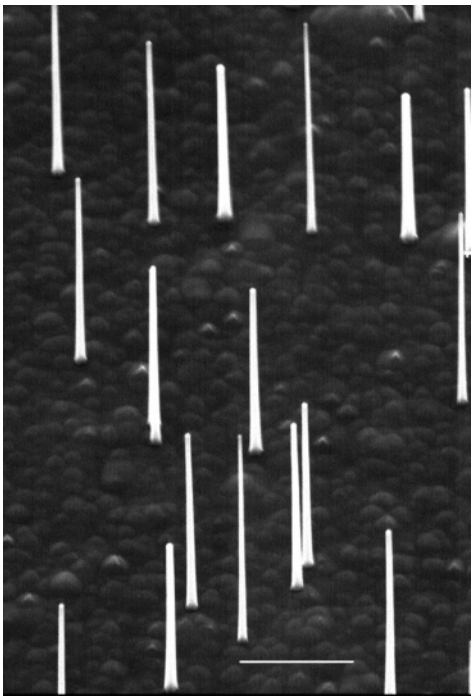

Figure 1. SEM image of GaP nanowires, grown on a (111)b GaP substrate from aerosol deposited catalytic gold particles. Tilt 45°, scale bar 1 μm.

For the nanowire samples, 2.5 μm high GaP nanowires were grown on GaP samples with a (111)B surface orientation. The samples were prior to growth pretreated by etching ($2HCl:2H_2O:1HNO_3$) and aerosol deposition of 50 nm gold particles (1 particle/μm^2)[27] (Figure 1). The details of nanowire growth and sample preparations have been described in detail in ref 28. Untreated glass cover slips and GaP substrates (hereafter called planar GaP) prepared without nanowire growth were used as comparative substrates. The substrates were sterilized in 70% ethanol and dried before use.

Nerve cells were obtained from adult mouse dorsal root ganglia (DRG). The DRG are part of the peripheral nervous system. They harbor the cell bodies of sensory neurons transmitting pain, temperature, and proprioceptive information to the central nervous system. The mice (NMRI, Möllegård, Denmark)) were anaesthetized and killed by heart puncture. The lumbar L6 DRG to the thoracic Th10 DRG were removed by dissection and dissociated in a solution of 0.25% collagenase as previously described.[29] The cells were suspended in serum-free RPMI 1640 culture medium to a concentration of approximately 300 nerve cells/μl. Cell suspension was then applied onto the dry substrates of GaP nanowires, planar GaP, and glass surfaces, respectively. The cells were allowed to settle for 5 min. Additional RPMI 1640 medium containing 10% fetal calf serum and nerve growth factor (42 ng/mL) was then added to stimulate neurite outgrowth. The cultures were maintained for 72 h at 37 °C in a humidified atmosphere of carbogen (6.5% CO_2 in O_2). During the dissociation process, the extracellular matrix and connective material between the cells in the ganglia are dissolved. Also, the nerve cells and the non-neuronal cells (mainly satellite cells, Schwann cells, fibroblasts, and epithelial cells) of the ganglia lose their processes and attain

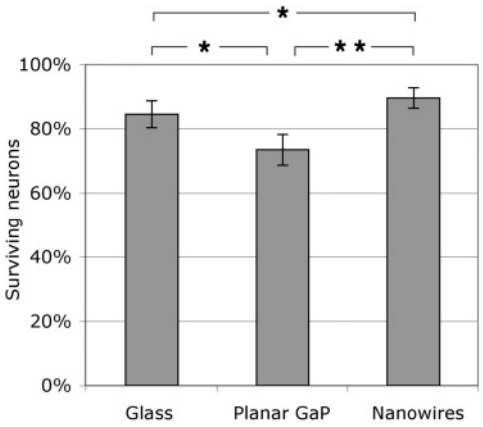

Figure 2. Nerve cell survival of cells cultured for 72 h on a GaP nanowires surface. Mean percentage of viable nerve cells adhered to different surfaces after 72 h culture [±SD $N = 5$]; *$p < 0.05$, **$p < 0.01$.

spherical morphology. When the cell dispersion is transferred to a culture substrate, a fraction of the cells successfully settle and adhere to the substrates, whereas nonadhering cells die. The adhering cells then attain a cell type dependent morphology (neurons being spherical or oval) and elaborate processes by reorganization of the cytoskeleton. The nerve cell processes, axons, can become several millimeters long. Most other cell types extend shorter processes and proliferate. These events continue as long as the cells remain viable and dissociated DRGs are a favorable, widely used system for studies of axonal outgrowth.

The adhesion of nerve cells was determined by counting the cells under a light (Normarsky) microscope. The number of nerve cells, distinguished from other cell types by their morphology and size, was counted on equal areas of the different substrates. The number of nerve cells adhered to the nanowire substrates (352 mm^{-2} SD 126) after 3 days of culturing was significantly higher than on glass (186 mm^{-2} SD 35.4, $p = 0.035$) and planar GaP (134 mm^{-2} SD 126, $p = 0.038$). The numbers were compared with the Student's t test, $n = 5$, using Bonferonis correction. Thus, more cells attached to the nanowire substrate than on the planar surfaces.

The viability of the nerve cells was accessed using the trypan blue dye exclusion method. The medium was exchanged for 1% trypan blue in phosphate buffered saline (PBS). After 5 min, the cultures were rinsed in RPMI 1640. The number of stained (dead or dying) and unstained (viable) neurons on each substrate was then counted. It was found that a substantial proportion of the nerve cells (>75%) was viable on all substrates. Figure 2 shows the average survival percentage (number of viable neurons divided by total number of neurons), with standard deviations, on glass, planar GaP, and GaP nanowires. The numbers were compared with the nonparametric Mann−Whitney U test. Statistical significances are shown in the graph (Figure 2). The results show that survival on GaP nanowires is as good as that on glass ($p < 0.05$) and significantly better than on planar GaP ($p < 0.01$). Thus, the nanowire substrate not only supports initial cell adhesion but also constitutes a substrate where the cells can survive and grow. Because the survival

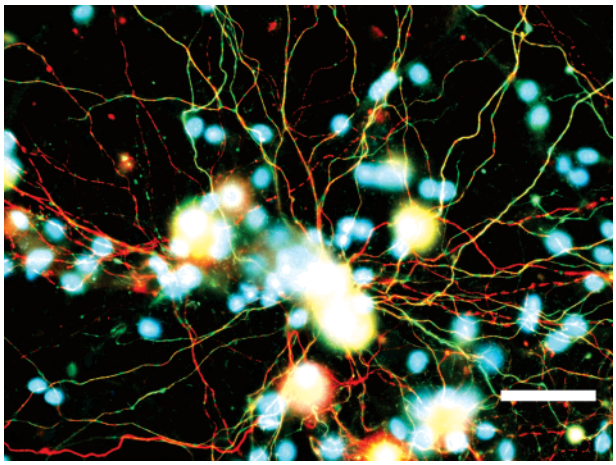

Figure 3. Fluorescence microscopy image of DRG-neurons cultured for 72 h on GaP nanowires. Neurofilaments and β III tubulin, both unique for neurons, are stained green and red, respectively. The nuclei of all cells are stained in blue with bisbenzimide. Note the large number of nerve cell processes. Scale bar 50 μm.

is lower on planar GaP, it is likely that the topography has this positive effect on cell survival. Improved adhesion is usually associated with improved survival. DRG neurons that detach do not survive in suspension. The nerve cell survival on GaP nanowires was also controlled using a 3-(4,5-dimethylthiazol-2-yl)-2,5-diphenyltetrazolium bromide (MTT) assay, which indicates respiratory activity of living cells. Cell cultures incubated for 72 h were treated with MTT (1 μg/mL). Nerve cells were observed before and 15 min after the MTT treatment. The numbers of viable (stained) and unviable (unstained) nerve cells were counted. The result (83.2%, SD 4.2%, $n = 4$) is in reasonable agreement with the numbers obtained from the trypan blue study (89.6%, SD 3.2%, $n = 5$).

The issue of neural outgrowth on the nanowire substrates was addressed by immunocytochemistry. Two neuron-specific antibodies, antineurofilament and antibeta III tubulin, were used. The preparations were counterstained with bisbenzimide to visualize cell nuclei. The cultures were fixed in Stefanini's fixative for 1 h and rinsed in PBS. They were then labeled with rabbit antibody to the 200 kD neurofilament subunit (1:200 dilution, Sigma) and a monoclonal anti-β-tubulin III antibody (1:400 dilution, Sigma) in 0.25% bovine serum albumin and 0.25% Triton X100 in PBS at 4 °C over night. After rinsing in PBS, secondary antibodies, Alexa Fluor 488, donkey-anti-rabbit, and Alexa Fluor 594, goat-anti-mouse (both 1:200 dilution, Sigma), were added for 2 h at room temperature. Cultures were then counterstained with bisbenzimide (1:1000 dilution, Sigma). The preparations were mounted and studied with an Olympus AX-70 fluorescence microscope.

Vigorous outgrowth of axons was observed on all substrates. Figure 3 shows an example of axonal outgrowth from cultures on GaP nanowires. Green color indicates neurofilament, and red color is related to β-tubulin immunoreactivity. The cytoskeletal staining pattern was characteristic of thriving neurons. The blue staining is bisbenzimide, which labels the nuclei of all cells including neurons, Schwann cells, fibroblasts, and satellite cells. As can be seen in Figure 3, axonal outgrowth from the neurons is abundant, indicating that the nerve cell thrive on the substrate during the 72 h of culturing.

The appearance of individual cells and their processes were also studied by scanning electron microscopy (SEM). The glass, planar GaP, and GaP nanowire cultures were dehydrated in ethanol, critical point dried (BAL-TEC CPD 030), and sputter coated with 5 nm gold/palladium (VG Microtech SC7640) before being analyzed in a Jeol JFM-6400F SEM.

On glass (Figure 4A), the non-neuronal cells often had a flattened well-spread morphology. Neurons could be distinguished by their typical large and round cell body and processes were abundant. On the planar GaP surface (Figure 4B), the non-neuronal cells were less flat and many cells had a spindle-shaped morphology. Cell aggregates were frequently observed in these cultures. The neurons appeared to have fewer processes. On the nanowire substrates (Figure 4C), the non-neuronal cells were spindle shaped. Neurons had rounded cell bodies and many processes. The morphology of the processes appeared different from that observed on planar GaP. On nanowires, the processes were not smooth but exhibited numerous filopodia attached to the nanowires. We assume that the nanowires can act as anchors for the cell, improving the adhesion to the substratum.

At higher magnifications, interactions between the nanowires and the cells became apparent. Despite the huge size difference between cells and wires (Figure 5A), the wires' effect on the cells was considerable. Most cell bodies were lying on top of the wires, penetrated by the uppermost part of the wires. Sometimes the cells rested directly on the surface, resulting in substantial wire penetration. Wires could be seen penetrating right through smaller cells (Figure 5B). Viable neurons (that is, neurons with extensive outgrowth and round cell bodies) were penetrated by nanowires. Whether the nanowires penetrate the cells by virtue of their thinness by a passive process as the cells land on them or whether the cells actively engulfs the nanowires by endocytosis upon encounter is still an open question. Cellular processes, on the other hand, are not present when the cells are deposited on the substrates, but evolve during the culturing. Therefore, their interactions with the nanowires must have formed in a slow, cell-controlled fashion. The SEM images showed that processes grew in three different ways, on top, at the bottom, or in between the nanowires (Figure 5D−F). Starting on top of the wires, many processes typically continued to grow attached to the wire tips for several μm. Some processes found their way down toward the surface at a shallow slope, apparently adhering to the wire sides during the descent. Once reaching the surface, processes stayed at that level and did not "climb" on top of the wires. At encounter, wires were either adhered to by thin sprouting filopodia or engulfed in a endocytosis-like manner. The close interaction between the wires and the cells resulted in an increased cell adherence. Moreover, the nanowires that attached to cell membranes had in many cases been bent by the cells and their processes (as in Figure 5B). This wire bending was in many cases very pronounced. Wires in

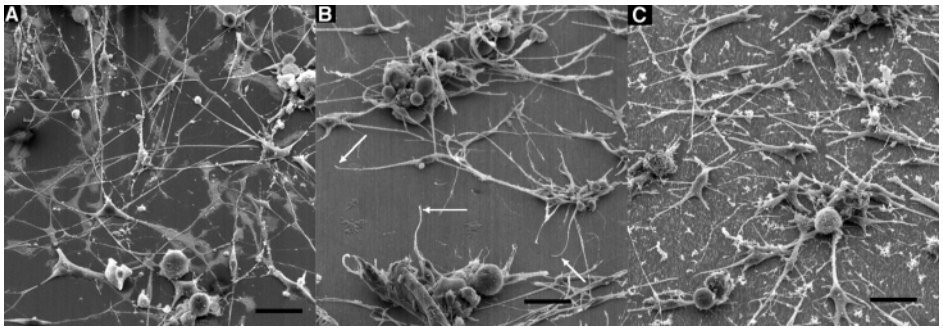

Figure 4. DRG-cells cultured 72 h on (A) glass, (B) planar GaP, and (C) GaP nanowires. Neurons have a spherical morphology and are endowed with axons. The non-neuronal cells and the processes, including axons, appear different on the three substrates. On glass (A) many non-neuronal cells are well-spread and flattened. At the planar GaP surface (B) the non-neuronal cells have a spindle shaped morphology and cell aggregates are abundant. The nanowire surface (C) shows axon morphology altered by the wires, with numerous filopodia. The nanowires are visible in the figure as the grainy-like background. Scale bars 25 μm.

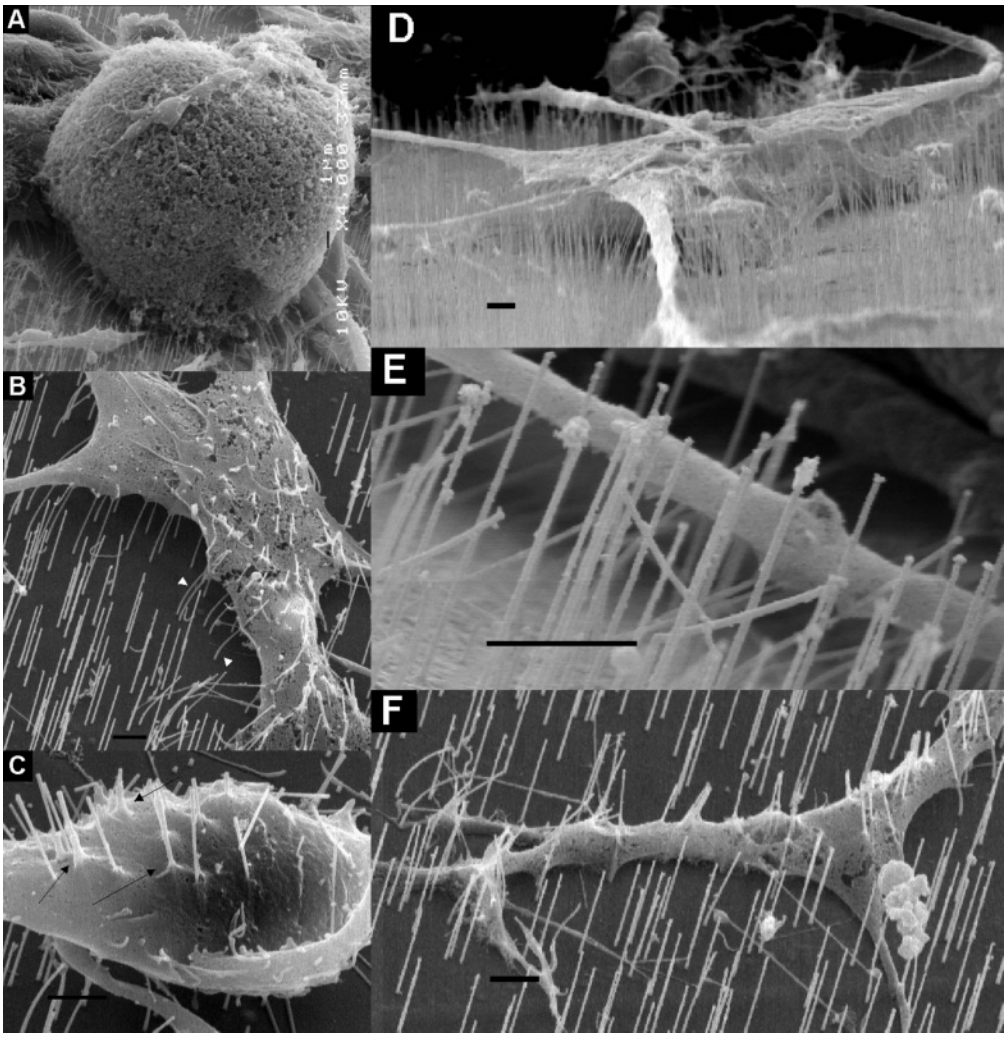

Figure 5. SEM-images showing interaction between nanowires and cells and cell processes. (A) Neural cell body on nanowires surfaces. (B) Well-spread non-neuronal cell penetrated by numerous nanowires. Note bending of the nanowires (white arrow heads). (C) Underside of cell body (mechically flipped over at rinsing) penetrated by nanowires. Note membrane adhesion to the nanowires (arrows). Figure 5 D−F demonstrate three different types of process growth. (D) Processes growing on top of the wires, attached to their tips. (E) Axon growing in the space between the substrate and the wire tips, adhering to the sides of the wires. (F) Process spreading over the bulk substrate, apparently engulfing nanowires encounterd along its path. Scale bars 1 μm.

contact with biological structures (for example, bent and engulfed wires) regularly appeared coated, most probably with membranes and proteins (arrows in Figure 5C).

Because it can be difficult to distinguish real phenomena from preparation artifacts from SEM observations, cultures were also investigated with confocal microscopy (Axiovert

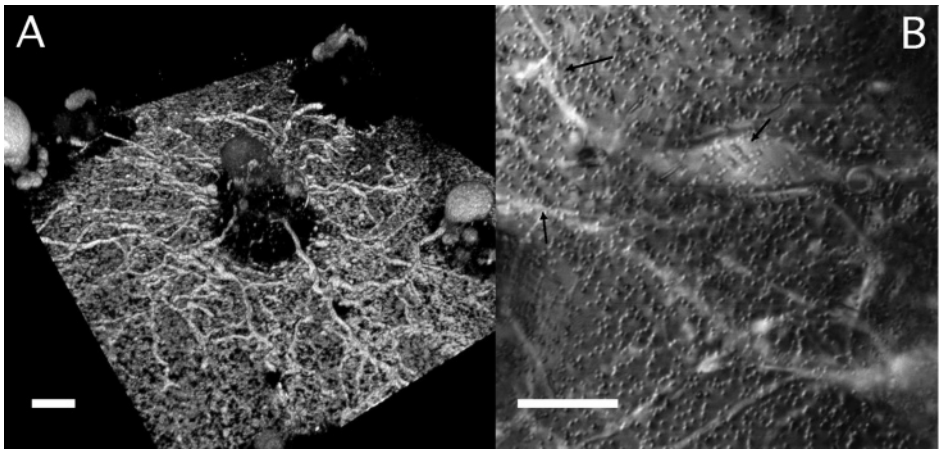

Figure 6. Confocal micrographs of GFP cells cultured on nanowires. (A) Three-dimensional perspective of nerve cells and axons. Nerve cell bodies raise above the surface, whereas the processes approaches the surface. (B) Thin slice, 1.0 μm, centered 0.5 μm above the surface of the substrate. Note the small cell bodies and their processes resting directly on the surface, penetrated by nanowires (black arrows). Scale bars 10 μm.

LSM 510, Zeiss) with a 40× 0.8 NA water immersion objective (Achroplan, Zeiss). Fluorescent-dissociated DRG cells from a green fluorescent protein (GFP) transgenic mouse (Okabe) were used in order to minimize destructive preparations such as staining and rinsing. Cells were cultured on nanowire substrates and fixated in the same way as described above. The substrates were placed upside-down on glass-bottom culture dishes (MatTek Corp., Ashald, MA) for investigation.

Individual 50 nm thick nanowires can be depicted with confocal microscopy, as they slightly scatter the laser light. With an optical slice of 1 μm, less than half the length of the wires, it was possible to determine the *z*-position of the cells relative to the wires. Single nanowires could be identified and the extreme proximity with the cells visualized.

The confocal images confirmed the SEM observations of cells lying on top of the wires (Figure 6A) or resting on the surface (Figure 6B). By looking at slices of cell bodies 0.5 μm above the surface, the presence of nanowires inside the cells was confirmed (Figure 6B).

Finally, simple patterns of nanowires were generated by using TEM grids as masks during the aerosol gold deposition ($1/\mu m^2$) preceding wire growth. The grids were mounted on the GaP samples with silver glue and were removed with hot acetone in an ultrasonic bath after aerosol deposition. This resulted in areas with wires and planar areas on the same sample. Dissociated DRG cells (from NMRI mouse) were cultured as described above but with the addition of 2% ECM gel (Sigma) dissolved in the medium to further improve cell adhesion to the planar surfaces. After 3 days, the cultures were fixed and prepared for SEM. The images showed that the cells did survive and extend processes on both types of areas. Processes from cells adhered to the nanowire areas reached the border and continued growing down to the planar surface. Processes of cells located on the planar areas could not grow up on, or into, the wire areas. Instead, they tended to follow the border between the two areas, creating a pattern as they grew (Figure 7). Thus, the nanowires acted to guide the growing nerve fibers.

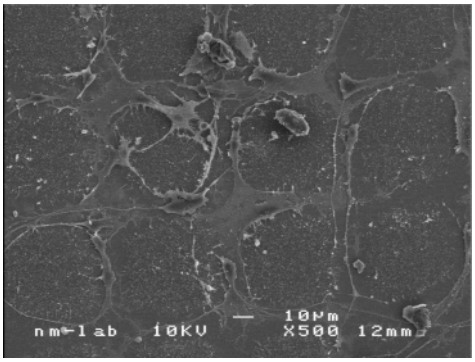

Figure 7. SEM image of cellular growth on a patterned nanowire substrate. Cell processes deriving from the wire areas can reach down to the planar surface, whereas processes growing on the planar surface cannot enter the dense wire areas. Instead they follow the flat area gridlike pattern.

We have shown that peripheral sensory neurons, and other cells from the DRG, can adhere, survive, and extend processes on GaP surfaces with GaP nanowires as well as on planar GaP surfaces. The cell adherence and cell survival on nanowire surfaces are as good as on untreated glass and better than on planar GaP. Nerve fibers can grow on top of and between the nanowires as well as on the basal substrate itself. The ultrafine diameters of the wires allow them to penetrate cells or to be engulfed by cells without the need of any external forces and without killing the cells. Moreover, forces exerted by the cells on the wires are observable in the SEM as wire bending. Patterned nanowire substrates generate patterned cell growth, as cells on the planar surfaces are unable to climb on top of the wires. These results show that vertical monolithic GaP nanowires are highly interesting structures for various cell culturing studies, including guiding of regenerating axons, probing cells (for example electrophysiological recordings) at extreme proximity, study of mechanotransduction, and possibly intracellular drug delivery. The ultrasmall dimensions of the wires and the possibility of creating arbitrary patterns of wires employing EBL and NIL enable spatial resolution orders of magnitude higher than that of conventional cell investigation techniques.

Note Added in Proof. During the review of our work a related paper was published by P. Yang and coworkers. Kim, W.; Ng, J. K.; Kunitake, M. E.; Conklin, B. R.; Yang, P. *J. Am. Chem. Soc.* **2007**, *129*, 7228.

Acknowledgment. The present study was supported by grants from the Swedish Research Council (VR), the Swedish Foundation for Strategic Research (SSF), the Swedish Agency for Technology and Innovation (VINNOVA), and the Øresund Academy. The confocal microscopy and image processing was performed at the Centre for Cellular Imaging at Gothenburg University. We thank Marie Adler (Cell and Organism Biology, Lund University) for dissection and cell culture expertise, Rita Wallén (Cell and Organism Biology, Lund University) for technical assistance with SEM preparations, and Maria Smedh and Julia Fernandez-Rodriguez (Center for Cellular Imaging, Göteborg Univesity) for education and support with the confocal microscopy.

References

(1) Clark, P.; Connolly, P.; Curtis, A. S. G.; Dow, J. A. T.; Wilkinson, C. D. W. *J. Cell Sci.* **1991**, *99*, 73.
(2) Curtis, A. S. G.; Casey, B.; Gallagher, J. D.; Pasqui, D.; Wood, M. A.; Wilkinson, C. D. W. *Biophys. Chem.* **2001**, *94*, 275.
(3) Dalby, M. J.; Berry, C. C.; Riehle, M. O.; Sutherland, D. S.; Agheli, H.; and Curtis, A. S. G. *Exp. Cell Res.* **2004**, *295*, 387.
(4) Bielen, J. A.; Schmidt, A.; Weiel, R.; Rutten, W. L. C. *Proceedings of the 18th Annual International Conference of the IEEE Engineering in Medicine and Biology Society*; Amsterdam, The Netherlands, October 31 to November 3, 1996; IEEE Engineering in Medicine and Biology Society: IEEE: Piscataway, NJ, 1997; p 2.
(5) Tan, J. L.; Tien, J.; Pirone, D. M.; Gray, D. S.; Bhadriraju, K.; Chen, C. S. *Proc. Natl. Acad. Sci. U.S.A.* **2003**, *100*, 1484.
(6) McKnight, T. E.; Melechko, A. V.; Hensley, D. K.; Mann, D. G. J.; Griffin, G. D.; Simpson, M. L. *Nano Lett.* **2004**, *4*, 1213.
(7) Zeck, G.; Fromherz, P. *Proc. Natl. Acad. Sci. U.S.A.* **2001**, *98*, 10457.
(8) Patolsky, F.; Timko, B. P.; Yu, G.; Fang, Y.; Greytak, A. B.; Zheng, G.; Lieber, C. M. *Science*. **2006**, *313*, 1100.
(9) Hutzler, M.; Lambacher, A.; Eversmann, B.; Jenkner, M.; Thewes, R.; Fromherz, P. *J. Neurophys.* **2006**, *96*, 1638.
(10) Flemming, R. G.; Murphy, C. J.; Abrams, G. A.; Goodman, S. L.; Nealey, P. F. *Biomaterials* **1999**, *20*, 573.
(11) Sniadecki, N. J.; Desai, R. A.; Ruiz, S. A.; Chen, C. S. *Ann. Biomed. Eng.* **2006**, *34*, 59.
(12) Gabay, T.; Jakobs, E.; Ben-Jacob, E.; Hanein, Y. *Physica A* **2005**, *350*, 611.
(13) Lovat, V.; Pantarotto, D.; Lagostena, L.; Cacciari, B.; Grandolfo, M.; Righi, M.; Spalluto, G.; Prato, M.; Ballerini, L. *Nano Lett.* **2005**, *5*, 1107.
(14) Gheith, M. K.; Sinani, V. A.; Wicksted, J. P.; Matts, R. L.; Kotov, N. A. *Adv. Mater.* **2005**, *17*, 2663.
(15) Matsumoto, K.; Sato, C.; Naka, Y.; Kitazawa, A.; Whitby, R. L. D.; Shimizu, N. *J. Biosci. Bioeng.* **2007**, *103*, 216.
(16) Lieber, C. M. *Sci. Am.* **2001**, *285*, 58.
(17) Mårtensson, T.; Carlberg, P.; Borgström, M.; Montelius, L.; Seifert, W.; Samuelson, *L. Nano Lett.* **2004**, *4*, 699.
(18) Björk, M. T.; Ohlsson, B. J.; Sass, T.; Persson, A. I.; Thelander, C.; Magnusson, M. H.; Deppert, K.; Wallenberg, L. R.; Samuelson, L. *Nano Lett.* **2002**, *2*, 87.
(19) Cui, Y.; Wei, Q.; Park, H.; Lieber, C. M. *Science.* **2001**, *293*, 1289.
(20) Wagner, R. S. In *Whisker Technology*; Levitt, A. P., Ed.; Wiley: New York, 1970; pp 47−119.
(21) Persson, A. I.; Samuelson, L.; Wallenberg, L. R. *Nat. Mater.* **2004**, *3*, 677.
(22) Dick, K. A.; Deppert, K.; Mårtensson, T.; Mandl, B.; Samuelson, L.; Seifert, W. *Nano Lett.* **2005**, *5*, 761.
(23) Mårtensson, T.; Svensson, C. P. T.; Wacaser, B. A.; Larsson, M. W.; Seifert, W.; Deppert, K.; Gustafsson, A.; Wallenberg, L. R.; Samuelson, L. *Nano Lett.* **2004**, *4*, 1987.
(24) Borgström, M.; Deppert, K.; Samuelson, L.; Seifert, W. *J. Cryst. Growth* **2004**, *260*, 18.
(25) Gallium Phosphide; MSDS; Electronic Space Products International: Ashland, OR, September 1995.*SPI Material Safety Data Sheet.* http://www.espi-metals.com/msds's/Gallium%20Phosphide.htm.
(26) Seifert, W.; Borgström, M.; Deppert, K.; Dick, K. A.; Johansson, J.; Larsson, M. W.; Mårtensson, T.; Sköld, N.; Svensson, C. T.; Wacaser, B. A.; Wallenberg, L. R.; Samuelson, L. *J. Cryst. Growth* **2004**, *272*, 211.
(27) Magnusson, M. H.; Deppert, K.; Malm, J-O.; Bovin, J-O.; Samuelson, L. *J. Nanoparticle Res.* **1999**, *1*, 243.
(28) Svensson, C. P. T.; Seifert, W.; Larsson, M. W.; Wallenberg, L. R.; Stangl, J.; Bauer, G.; Samuelson, L. *Nanotechnology* **2005**, *16*, 936.
(29) Lindwall, C.; Dahlin, L.; Lundborg, G.; Kanje, M. *Mol. Cell. Neurosci.* **2004**, *27*, 267.

NL070728E